Relaxation Kinetics of Cytochrome P450 Reductase: Internal Electron Transfer Is Limited by Conformational Change and Regulated by Coenzyme Binding†

Aldo Gutierrez,‡ Mark Paine,§ C. Roland Wolf,§ Nigel S. Scrutton,*,|| and Gordon C. K. Roberts*,‡

Biological NMR Centre, University of Leicester, Medical Sciences Building, P.O. Box 138, University Road, Leicester LE1 9HN, U.K., Department of Biochemistry, University of Leicester, University Road, Leicester LE1 7RH, U.K., and Biomedical Research Centre, University of Dundee, Ninewells Hospital and Medical School, Dundee DD1 9SY, U.K.

Received November 14, 2001; Revised Manuscript Received February 12, 2002

ABSTRACT: The kinetics of internal electron transfer in human cytochrome P450 reductase have been studied using temperature-jump relaxation spectroscopy. Temperature perturbation of CPR reduced at the two-electron level with NADPH yields biphasic absorption transients at 450 and 600 nm. The observed rate, $1/\tau$, for the fast phase is 2200 ± 300 s^{-1}. The absence of this phase in fluorescence transients and in absorption transients collected with dithionite-reduced enzyme indicates this phase does not report on electron/hydride transfer and is consistent with its origin in local conformational change in the vicinity of the FAD isoalloxazine ring. The slow phase ($1/\tau = 55 \pm 2$ s^{-1}) observed in the absorption transients obtained with CPR reduced at the two-electron level with NADPH reports on internal electron transfer: $FAD_{sq}-FMN_{sq} \rightarrow FAD_{ox}-FMN_{hq}$. The observed rate of this transient is slower ($1/\tau = 11 \pm 0.5$ s^{-1}) in CPR reduced to the two-electron level by dithionite rather than NADPH, demonstrating that coenzyme binding has an important influence on the observed rate of internal electron transfer. Temperature perturbation experiments with CPR reduced with 10-fold molar excess of NADPH produce monophasic absorption transients ($1/\tau = 20 \pm 0.2$ s^{-1}) reporting on internal electron transfer: $FAD_{sq}-FMN_{hq} \rightarrow FAD_{hq}-FMN_{sq}$. The observed rate constants for electron transfer are substantially less than those expected from analysis of CPR by electron-transfer theory ($\sim 10^{10}$ s^{-1}). Potential gating mechanisms have been investigated using the temperature-jump method. Observed rates for electron transfer were unaffected in experiments performed in deuterated solvent, indicating that deprotonation does not gate the reaction. Introduction of glycerol into the sample significantly decreased the observed rate for internal electron transfer, suggesting conformational gating of the reaction. Replacement of Trp-676 with His-676 reduces ~2-fold the observed rate of internal electron transfer in two-electron-reduced enzyme, whereas the observed rate for $FAD_{sq}-FMN_{hq} \rightarrow FAD_{hq}-FMN_{sq}$ transfer is increased approximately 13-fold in the W676H mutant reduced with a 10-fold molar excess of NADPH. The studies reveal altered redox properties of the FAD in W676H CPR. The data are discussed in the context of previous stopped-flow studies of human CPR and the X-ray crystallographic structure of rat CPR.

The cytochrome P450 enzymes are a superfamily of heme-containing monooxygenases that hydroxylate a wide range of physiological and xenobiotic compounds (*1*). In eukaryotic cells, type II cytochromes P450 are located in the endoplasmic reticulum, where they receive electrons from the diflavin enzyme cytochrome P450 reductase (CPR; EC 1.6.2.4)[1] (*1*−*5*). CPR catalyzes electron transfer from NADPH, an obligatory two-electron donor, to the P450 cytochromes. The monooxygenation reaction catalyzed by these enzymes is dependent on a finely coupled stepwise supply of electrons. CPR is a 78 kDa membrane-bound flavoprotein containing one molecule each of FMN and FAD (*6*). It is likely to have evolved by the fusion of two ancestral genes encoding proteins related to ferredoxin−$NADP^+$ reductase (FNR) and flavodoxin (Fld) (*7*), bringing the two flavins in close proximity for efficient electron transfer (Figure 1). The enzyme also transfers electrons to cytochrome b_5 (*8*), heme oxygenase (*9*), and the fatty acid elongation system (*10*). CPR can also reduce a number of artificial redox acceptors (*11, 12*) and drugs (*13*−*17*), and may also have a role in the generation of reactive oxygen species in the cell.

CPR is a member of a growing family of mammalian diflavin reductases, which includes the isoforms of nitric oxide synthase (*18*), methionine synthase reductase (*19*), and protein NR1 (*20*). Unlike ferredoxin−$NADP^+$ reductase, which catalyzes the reduction of $NADP^+$ to NADPH, in vivo the diflavin reductases catalyze the oxidation of NADPH. However, our recent kinetic studies of 'reverse' electron transfer in the isolated FAD domain of human CPR indicate that electron transfer in the nonphysiological direction (i.e., formation of NADPH) is faster than that in the physiological

† This work was funded by grants from the MRC, the Lister Institute of Preventive Medicine, and the Wellcome Trust. N.S.S. is a Lister Institute Research Fellow.

* Corresponding authors. N.S.S.: Telephone, +44 116 223 1337; Fax, +44 116 252 3369; Email, nss4@le.ac.uk. G.C.K.R.: Telephone, +44 116 252 2978; Fax, +44 116 223 1503; Email, gcr@le.ac.uk.

‡ Biological NMR Centre, University of Leicester.

§ Biomedical Research Centre, University of Dundee.

|| Department of Biochemistry, University of Leicester.

[1] Abbreviation: CPR, cytochrome P450 reductase.

10.1021/bi0159433 CCC: $22.00
Published on Web 03/09/2002

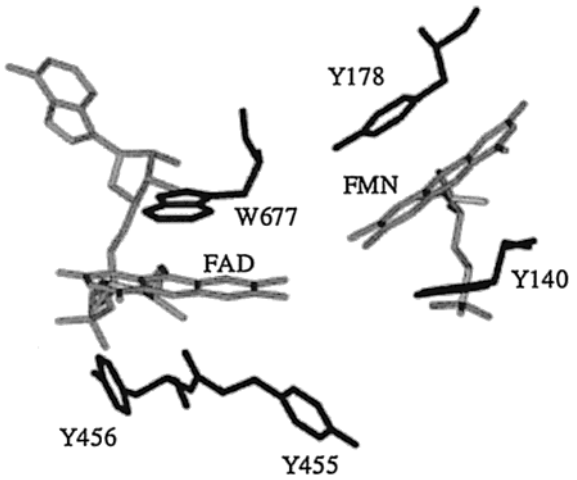

FIGURE 1: Relative positions of the flavins (FAD and FMN) and their immediate environment in the X-ray crystal structure of oxidized rat CPR (*7*).

oxidation of NADPH (*21*). These findings are consistent with the known reduction potentials of the FAD domain (*22*). The high potential of the $FMN_{ox/sq}$ couple [−66 mV (*22*)] provides a rationale for the ability of full-length CPR to catalyze NADPH oxidation, since following oxidation of NADPH, there is a large driving force for the transfer of one electron from FAD_{hq} to FMN_{ox}.

Stopped-flow kinetic and potentiometric studies have provided a detailed understanding of the overall kinetic mechanism of electron transfer in CPR (*21*−*24*). However, owing to the relatively slow rate of flavin reduction, the internal electron transfer between the flavins cannot be studied using the stopped-flow method, since internal electron transfer is limited by the preceding hydride-transfer event. In this paper, we describe the use of a relaxation kinetic method based on temperature-jump technology to investigate the kinetics of internal electron transfer, thus relieving us of the constraints imposed by the stopped-flow method. We have studied internal electron transfer in two- and three-electron-reduced CPR and shown the reaction to be relatively slow. We provide evidence for conformational gating of internal electron transfer, and we show that mutation of Trp-676 has a major effect on the kinetics of internal electron transfer in both the 'forward' and 'reverse' directions.

EXPERIMENTAL PROCEDURES

Materials. Deuterium oxide (≥99.9% ^2H) was purchased from Goss Scientific Instruments, U.K. NADPH, sodium dithionite, methyl viologen, FAD, and FMN were from Sigma. All other chemicals were of analytical grade.

Protein Purification. Human fibroblast CPR (lacking the N-terminal membrane-anchoring region) and the corresponding W676H mutant were expressed in *Escherichia coli* strain BL21(DE3)pLysS from plasmid pET15b, and purified as described previously (*21, 24*).

Temperature-Jump and Stopped-Flow Kinetic Methods. Stopped-flow kinetic experiments were performed under anaerobic conditions as described previously (*21, 24*). Temperature-jump kinetic experiments were carried out using a TJ-64 temperature-jump instrument (Hi-Tech Scientific). The heating time was 4 μs as measured using a standard phenolphthalein−glycine buffer test (*25*). The TJ-64 model is equipped with a parallel-plate capacitor with a storage capacitance of 0.04 μF. The power output used throughout this study was 12.5 kV, which gives a temperature rise of approximately 7 °C. The starting temperature was set at 20 °C using a refrigerated circulating bath (model RB-5A, Techne) attached to the cell block thermostat chamber. After each temperature-jump acquisition, the sample content of the cell was manually exchanged, and 1 min was allowed to elapse for the cell to cool back to its thermostat temperature. Room temperature was 20 °C, thus maintaining samples at a constant temperature during exchange from the optical cell block. To maximize the signal-to-noise ratio, a relatively high protein concentration was required (140 μM). Prior to enzyme reduction, all protein samples were treated with potassium hexacyanoferrate, and excess cyanoferrate was removed by rapid gel filtration (Sephadex G25). Reduced CPR samples were prepared in an anaerobic glovebox (Belle Technology Ltd.) as described elsewhere (*21*). On reducing CPR with the appropriate reductant (NADPH or sodium dithionite), the sample was allowed to equilibrate until no further spectral change was observed. The sample was then transferred anaerobically to the optical cell of the temperature-jump apparatus, from gastight syringes attached to the cell block via a series of Luer connectors. Prior to introduction of the sample, the cell was made anaerobic by flushing with a concentrated solution of sodium dithionite followed by extensive flushing with anaerobic buffer. Measurements were carried out in 100 mM potassium phosphate buffer, pH 7.0. All buffers were made oxygen-free by evacuation and bubbling with argon prior to placement in the anaerobic glovebox. Standardized sodium dithionite solutions (approximately 15 mM) were prepared daily by addition of 100 mM potassium phosphate buffer, pH 7.0, to preweighed amounts of solid sodium dithionite (8−15 mg). The concentration of the solution was calculated by titration against a standard solution of FAD (100 μM; $\epsilon_{450} = 11\,300\ M^{-1}\ cm^{-1}$) using methyl viologen as an indicator. Preweighed solid sodium dithionite was kept under N_2, protected from light and humidity.

Absorbance measurements in the temperature-jump apparatus were made using a 100 W tungsten lamp coupled to a monochromator, while a 75 W xenon−mercury lamp was used for fluorescence measurements. The excitation wavelength employed for tryptophan fluorescence studies was 297 nm (297FS10-25 filter, Andover Corp.) in combination with a WG 320 cutoff emission filter (Oriel Instruments, #51255). For measurement of NADPH fluorescence, the excitation wavelength was 365 nm (365FS10-25 filter, Andover Corp.), and emission was measured using a GG420 nm filter (Oriel Instruments, #51280). To prevent photobleaching, samples were protected from the incident light during the cooling time. Typically, 20 transients were collected and averaged for each reaction condition. Observed rates of approach to the new equilibrium position were calculated by fitting transients using the software package of the t-jump system.

Solvent Isotope Effect Studies. Potassium phosphate buffer solutions were lyophilized and resuspended in 99.9% ^2H_2O. The p^2H was taken as the apparent (measured) pH + 0.41, to compensate for the deuterium isotope effect on the glass electrode. Where required, the p^2H was adjusted with NaO^2H. Buffers were made anaerobic by evacuation and extensive

bubbling with ^2H_2O-saturated argon. Oxidized CPR samples were placed in the anaerobic glovebox and exchanged into the appropriate buffer by gel filtration using Sephadex G-25 columns that had been swollen and preequilibrated with 99.9% ^2H_2O−potassium phosphate buffer (p^{2}H = 6.5, 7.0, or 7.5). The protein was kept overnight (~12 h) under an atmosphere of nitrogen at 4 °C to allow deuterium exchange. CPR was reduced to the two-electron level by titration with dithionite solution. Sodium dithionite solutions were prepared as described above using 99.9% ^2H_2O−potassium phosphate buffer, p^{2}H 7.0.

Solvent Viscosity Effect. Glycerol was used as viscosogen. The magnitude of the temperature jump is dependent on the heat capacity (C_p) of the solution (see below). Therefore, adjustments to the voltage output were needed to compensate for the heat capacity difference between water [4.18 J/(g·°C)] and glycerol [2.39 J/(g·°C)]. The energy stored in a capacitor is given by

$$H = 0.5CV^2 \quad (1)$$

where C is the capacitance (0.04 μF) and V is the voltage across the plates (normally 12.5 kV). This energy is related to the heating of the sample by the standard equation for heat transfer:

$$H = mC_p\Delta T \quad (2)$$

where m is the mass (g), C_p is the heat capacity [J/(g·°C)], and ΔT is the temperature variation (°C). The relative contribution of the protein to the heat capacity of the solution is practically negligible, so C_p and m refer to the solvent. Thus, the temperature-jump in the cell upon capacitor discharge is given as

$$\Delta T = \frac{0.5CV^2}{\rho C_p \nu} \quad (3)$$

where m is now expressed as $\rho\upsilon$, ρ being density (g/mL), and υ is the cell volume (0.1 mL). The high density of glycerol (1.3 g/mL) in relation to water (0.99 g/mL) partially compensates for the difference in heat capacity values ($[\rho C_p]_{water} = 0.74[\rho C_p]_{glycerol}$). Equation 3 predicts a temperature-jump of 10 °C at 100% glycerol (cf. 7 °C when water is the solvent). Consequently, only small adjustments in the voltage output were required to keep the magnitude of the temperature-jump constant (7 °C) at different concentrations of glycerol (e.g., 10.7 kV at 75% glycerol).

RESULTS

Equilibrium States in Chemical Relaxation Reactions with Two-Electron-Reduced CPR. The interpretation of temperature-jump kinetic transients relies on knowledge of the equilibria involved. This is potentially difficult with CPR where initial fast reduction by excess NADPH in stopped-flow studies is followed by slow thermodynamic relaxation, leading to an equilibrium mixture of several different redox forms of CPR. These latter enzyme species arise from a series of disproportionation reactions following enzyme reduction, which have been observed in both rabbit and human CPR (*21*, *23*). In stopped-flow studies with excess NADPH, unequivocal identification of the enzyme species in the final equilibrium state is therefore difficult. In the temperature-jump relaxation studies reported here, the experimental conditions were selected to minimize the uncertainty arising from the identity of the enzyme species in this final equilibrium. Rapid mixing of human CPR with stoichiometric NADPH yields a kinetic transient at 600 nm in which the major absorption change occurs within 50 ms of mixing. This transient describes the formation of a ~50:50 equilibrium mixture of the blue di-semiquinoid species (FAD_{sq}/FMN_{sq}) and the FMN hydroquinone species (FAD_{ox}/FMN_{hq}) of CPR. The stability of this mixture of enzyme species is apparent from the lack of further significant absorption change beyond 50 ms. The equilibrium distribution in two-electron-reduced enzyme reflects the redox potential values determined recently for human CPR [Figure 2B; (*22*)]. The high-potential blue semiquinone species of the FMN ($FMN_{ox/sq} = -66$ mV) provides the driving force for interdomain electron transfer following hydride transfer from NADPH to FAD. The FAD

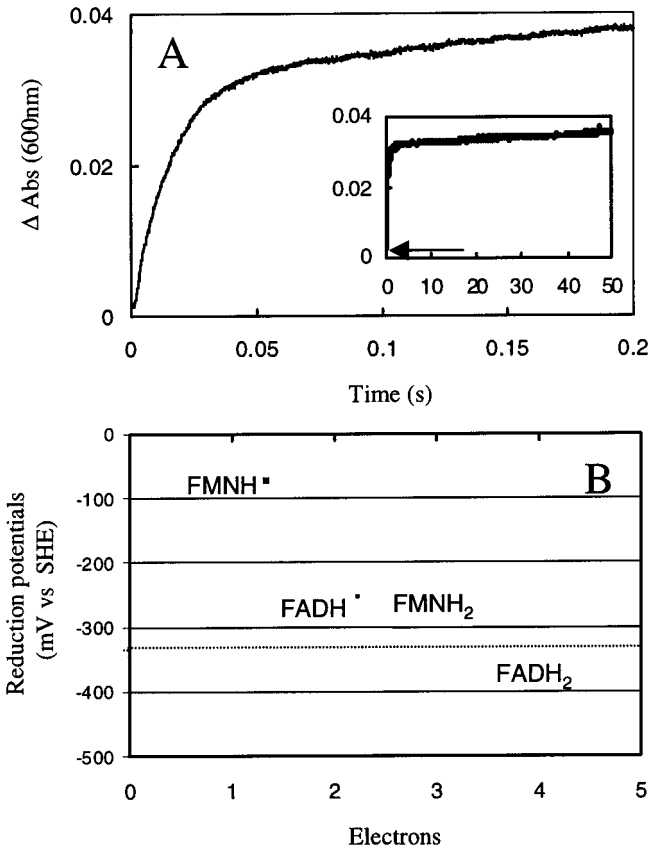

FIGURE 2: Formation of the blue di-semiquinone species of human CPR in rapid-mixing experiments and the midpoint reduction potentials of human CPR. Panel A: kinetic transient at 600 nm from a rapid-mixing stopped-flow experiment involving the reduction of CPR by a stoichiometric amount of NADPH. Conditions: 10 μM CPR, 100 mM potassium phosphate buffer, pH 7.0, 25 °C. Formation of the blue di-semiquinone species is complete within the first 50 ms. Data are best described by a double exponential function, yielding values for k_{obs1} and k_{obs2} of 72 s^{-1} (blue di-semiquinone formation) and 4 s^{-1} (unassigned small absorption changes that may represent a small amount of disproportionation), respectively. Inset: longer time base trace for the same reaction, showing that further absorption changes are minimal. Panel B: reduction potentials for the flavin cofactors in CPR. Midpoint reduction potentials values are from (*22*): $FMN_{ox/sq} = -66$ mV, $FAD_{ox/sq} = -283$ mV, $FMN_{sq/hq} = -269$ mV, and $FAD_{sq/hq} = -380$ mV. The hatched line indicates the reduction potential for the $NADP^+$/NADPH couple (−320 mV).

Scheme 1

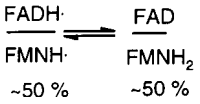

blue semiquinoid species that is formed following this internal electron transfer is approximately isopotential with the $FMN_{sq/hq}$ couple ($FAD_{ox/sq} = -283$ mV; $FMN_{sq/hq} = -269$ mV), thus poising the equilibrium distribution at ~50% of each species. Temperature-jump perturbation of this equilibrium will lead to further and transient oxidation of the FAD, thus increasing the concentration of the FAD_{ox}-FMN_{hq} species (Scheme 1); the very low potential of the $FAD_{sq/hq}$ couple (−380 mV) would prevent reverse electron transfer to yield a species containing $FADH_2$/FMN.

To prepare CPR for temperature-jump experiments, we reduced the enzyme either with the physiological reductant NADPH or with the artificial reductant sodium dithionite. Spectra obtained during static titration of CPR under anaerobic conditions confirmed that the equilibrium distribution of enzyme species is equivalent for both reductants, indicating that the potentials of the flavin couples are not influenced by the nature of the reductant (Figure 3).

Kinetic Transients and Data Processing. A major problem of the temperature-jump method is the potential for additional optical signals to be superimposed on the true relaxation transient (*26*, *27*). These additional signals are attributable to pressure pulse propagation (*28*) and electric linear dichroism (*29*) effects owing to sudden thermal heating and high voltage through the cell, respectively. These effects were identified through the use of appropriate control measurements. Apparent absorption increases were observed following temperature-jump reactions performed with buffer alone (Figure 4A) and oxidized CPR contained in buffer (Figure 4B). Relaxation transients obtained with two-electron-reduced CPR exhibited an additional reduction in absorption as an initial phase prior to the signal increase observed in reactions with either buffer alone or oxidized CPR (Figure 4C). This new kinetic information was recovered by subtraction of the signal observed for oxidized CPR (Figure 4D). This transient shows 'up−down' behavior; the slower 'down' phase is described by a single-exponential process ($1/\tau = 55 \pm 2$ s^{-1}) and is preceded by a more rapid 'up' phase ($1/\tau = 2200 \pm 300$ s^{-1}; Figure 4D), analysis of which is simplified by using a shorter time base (10 ms; Figure 4E,F). The absorption signals returned to the baseline level (i.e., the level prior to discharge of the capacitor) following an appropriate cooling period (30−40 s), thus demonstrating the reversibility of the system (data not shown). In all temperature-jump experiments employing new conditions (e.g., inclusion of glycerol), control temperature-jumps were performed with oxidized CPR under the same conditions. For studies of internal electron transfer, data were processed to generate difference absorption transients by subtracting the transient obtained for the oxidized enzyme from that obtained for reduced CPR.

Assignment of the Kinetic Phases. Our first temperature-jump experiments were performed with CPR reduced at the two-electron level by NADPH. Temperature-jump kinetic transients were monitored at both 450 and 600 nm (Figure 5A,C); the former wavelength reports on the oxidation level

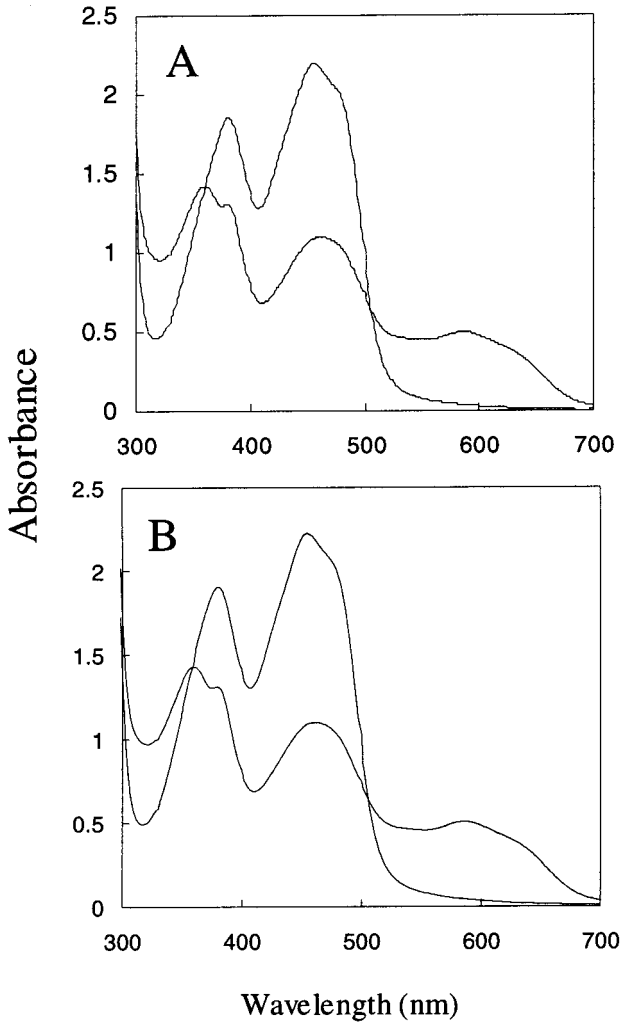

FIGURE 3: Absorption spectra of two-electron-reduced CPR. Panel A: spectrum obtained after reduction of human CPR with a stoichiometric amount of NADPH. Conditions: 140 μM CPR, 100 mM potassium phosphate buffer, pH 7.0. The reaction was carried out under anaerobic conditions. The sample was allowed to equilibrate until no further spectral changes were observed. Panel B: spectrum obtained after reduction of the enzyme with 2 electron equivalents using sodium dithionite (previously titrated against a standard solution of FAD). Conditions: as for panel A.

of the flavins and the latter on the presence of blue semiquinone. Identical rates for the 'down' phase were observed at both wavelengths ($1/\tau = 55 \pm 11$ s^{-1}), suggesting both wavelengths report on the same kinetic process. The amplitude changes at 600 nm were much smaller, owing to the small extinction coefficients for the blue flavin semiquinones at this wavelength, as reported in our recent stopped-flow studies (*21*). This observed rate ($1/\tau = 55 \pm 11$ s^{-1}) is similar to that attributed to interdomain electron transfer in rat CPR (70 s^{-1}) measured using flavin photochemistry (*30*). The loss of absorption at 600 nm in the 'down' phase of the transient is consistent with conversion of the di-semiquinoid form of CPR to a form containing oxidized FAD and hydroquinone FMN. We therefore attribute this kinetic phase to internal electron transfer from FAD_{sq} to FMN_{sq} to form FAD_{ox} and FMN_{hq}; this is consistent with Scheme 1. The rate observed with dithionite-reduced CPR is 5 times less ($1/\tau = 11 \pm 0.5$ s^{-1}; Figure 5B) than the corresponding value for NADPH-reduced CPR, despite the fact that the position of the initial equilibrium is the same

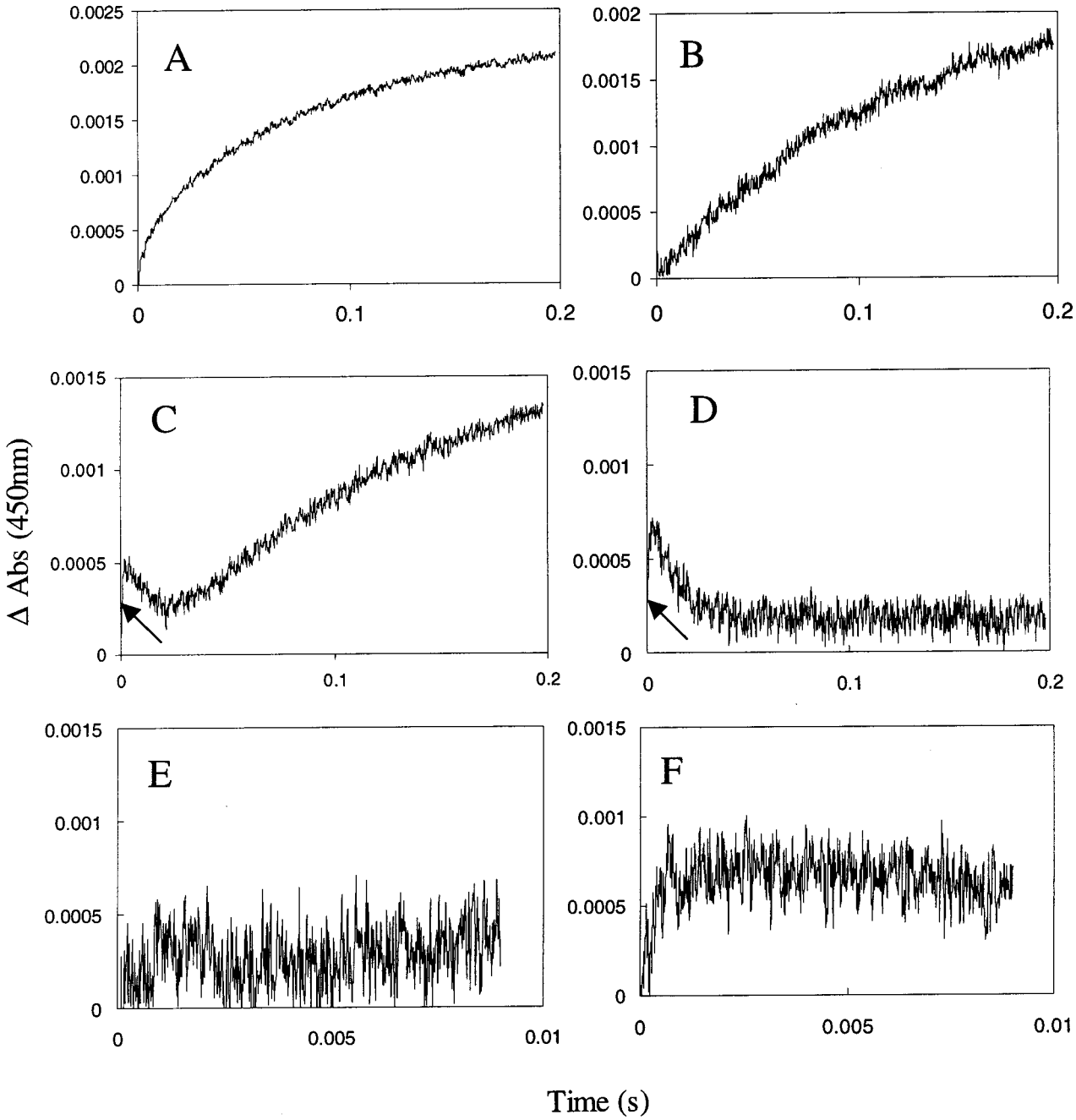

FIGURE 4: Temperature-jump kinetic transients and data processing. Conditions: thermostat temperature, 20 °C; temperature-jump, +7 °C; voltage discharge, 12.5 kV; 140 μM CPR, 100 mM potassium phosphate buffer, pH 7.0. All panels are absorption transients recorded at 450 nm. Panel A: transient observed following capacitor discharge through the cell containing only 100 mM phosphate buffer, pH 7.0. Panel B: transient observed following capacitor discharge through the cell containing oxidized CPR. Panel C: transient observed following capacitor discharge through the cell containing CPR reduced at the two-electron level by NADPH; note the two new initial phases not seen in panels A and B. Panel D: difference transient (transient C minus transient B) for two-electron-reduced CPR. The 'down' phase is best fitted to a single-exponential expression ($1/\tau = 55 \pm 2$ s^{-1}). On a shorter time base (10 ms), the difference transient reports solely on the initial fast 'up' phase ($1/\tau = 2200 \pm 300$ s^{-1}). Panel E: as for panel B, but over a 10 ms time base. Panel F: as for panel C, but over a 10 ms time base. Arrows indicate the absorption at the point of data acquisition.

in both cases (Figure 3). The difference in observed rate most probably arises from the conformational changes that occur in the region of the FAD domain on binding NADPH, particularly in the region of Trp-676 (*24*).

As with the 'down' phase, the faster 'up' phase seen at 450 nm (Figure 4D,F) is also seen at 600 nm ($1/\tau = 1800 \pm 200$; Figure 6A). This 'up' phase is absent from transients obtained with dithionite-reduced CPR (Figure 6B), raising the possibility that the signal might be attributed to a nicotinamide−flavin charge-transfer species. NADPH−FAD charge-transfer intermediates have been observed in our previous stopped-flow studies of human CPR (*21*). The optical signature of the NADPH−FAD charge-transfer complex seen in our stopped-flow studies is broad, exhibiting increased absorption in the region 500−700 nm. We have thus performed temperature-jump experiments and collected transients in the range 500−700 nm to investigate the possible formation of an NADPH−FAD charge-transfer intermediate by reverse electron transfer from $FADH_2$.[2] However, the transients collected over this wavelength range

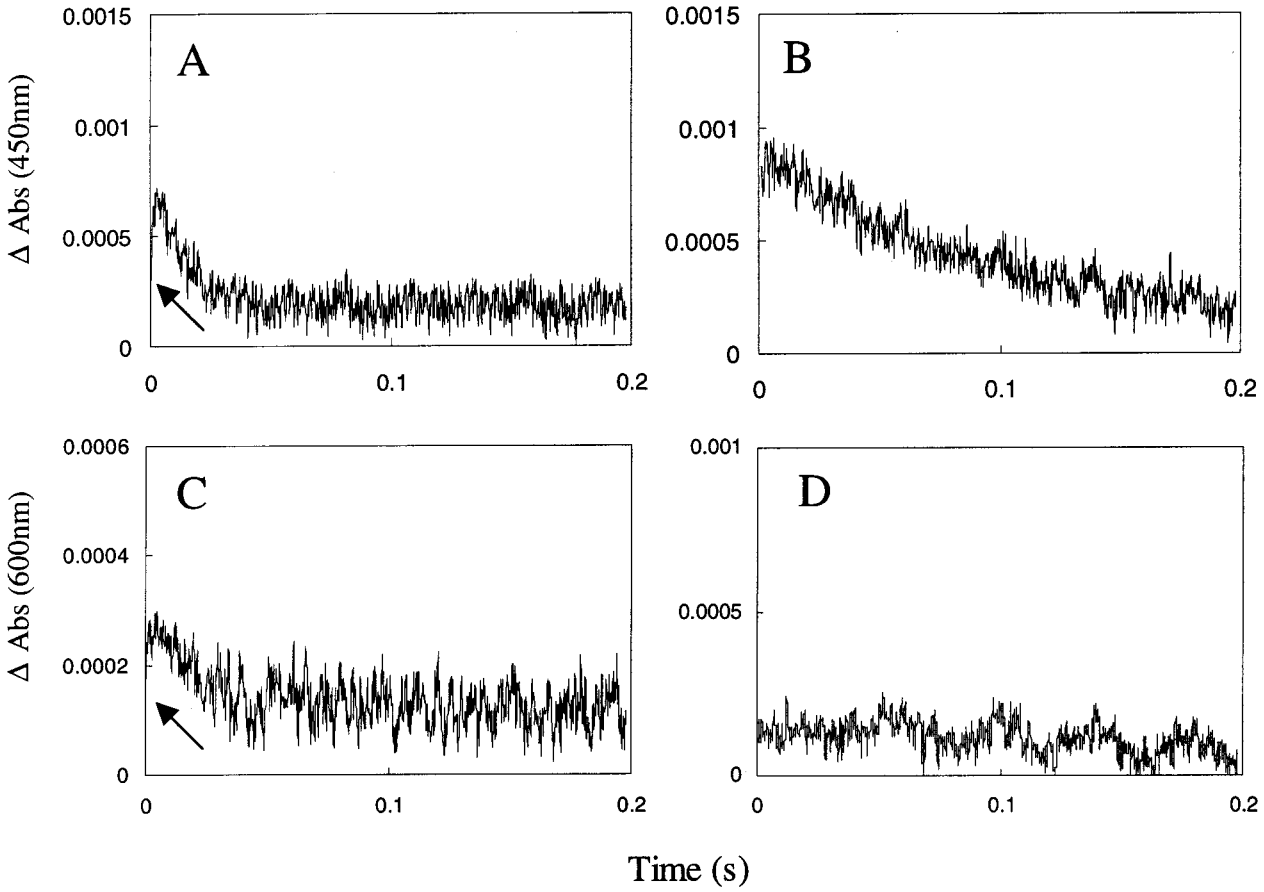

FIGURE 5: Temperature-jump difference absorption transients obtained for CPR reduced at the two-electron level with NADPH and sodium dithionite. Conditions: 140 μM CPR, 100 mM potassium phosphate buffer, pH 7; temperature-jump as for Figure 4. Panel A: difference absorption transient measured at 450 nm for CPR reduced with NADPH; for the 'down' phase, $1/\tau = 55 \pm 2$ s^{-1}. Panel B: difference absorption transient measured at 450 nm for CPR reduced with sodium dithionite; for the 'down' phase, $1/\tau = 11 \pm 0.5$ s^{-1}. Panel C: difference absorption transient measured at 600 nm for CPR reduced with NADPH; for the 'down' phase, $1/\tau = 55 \pm 11$ s^{-1}. Panel D: as for panel B, but monitoring at 600 nm. Arrows indicate the absorption at the point of data acquisition.

generated a kinetic difference spectrum that is characteristic of the flavin blue semiquinone rather than of a NADPH−FAD charge-transfer species (Figure 6C, inset).

We exclude the possibility that the 'up' phase represents electron transfer between the flavins on a number of grounds. The first is based on the measured potentials which, as discussed above, would require the movement of an electron 'uphill' from $FMNH_2$ to FAD. This is counterintuitive, and on this basis alone, we can reject this interpretation. Further evidence is provided by the key observation that the 'up' phase observed with stoichiometric NADPH is retained in temperature-jump experiments performed with excess nicotinamide cofactor (e.g., stoichiometric NADPH plus 10-fold excess $NADP^+$ or 10-fold NADPH plus 10-fold $NADP^+$; Figure 6D,C, respectively). Under these conditions, the initial position of the equilibrium is different from that for two-electron-reduced CPR (Figure 6D, inset), but despite this the 'up' phase is retained over 10 ms in temperature-jump experiments. By contrast, the fast 'up' phase is not observed in temperature-jump transients obtained with enzyme reduced to the two-electron level by dithionite, notwithstanding the fact that in this case the position of the equilibrium is very similar to that obtained by addition of stoichiometric NADPH. These findings clearly show that the 'up' phase observed with nicotinamide-reduced enzyme does not represent electron transfer; we suggest that it represents a nonreductive change in the environment of one or both of the bound flavins, which enhances the absorption properties of the blue flavin semiquinone(s).

NADPH fluorescence measurements do not show any changes in the oxidation state of the nicotinamide cofactor during equilibrium perturbation over both short (10 ms) and longer (0.2 s; data not shown) time bases, again ruling out reverse electron transfer from $FADH_2$ to $NADP^+$. In stopped-flow studies, we have shown previously that formation of the EH_2−$NADP^+$ intermediate immediately following hydride transfer to FAD triggers changes in the fluorescence properties of Trp-676, which is located close to the FAD isoalloxazine ring (*24*). However, in temperature-jump experiments, changes in tryptophan fluorescence do not accompany the transient relaxation of the system (data not shown). These observations argue against the formation of any charge-transfer complex (NADPH−FAD or $NADP^+$−$FADH_2$) in our temperature-jump studies, but favor the interpretation that the spectral changes observed in the 'up' phase are associated with the absorption properties of the flavin cofactors alone. We infer, therefore, that the equilib-

[2] Although formally we have to consider this possibility, from the outset we considered reverse electron transfer from $FADH_2$ to $NADP^+$ to be unlikely. This arises owing to the low potential of the $FAD_{sq/hq}$ couple, which indicates that the FAD hydroquinone is very poorly populated at equilibrium in two-electron-reduced CPR.

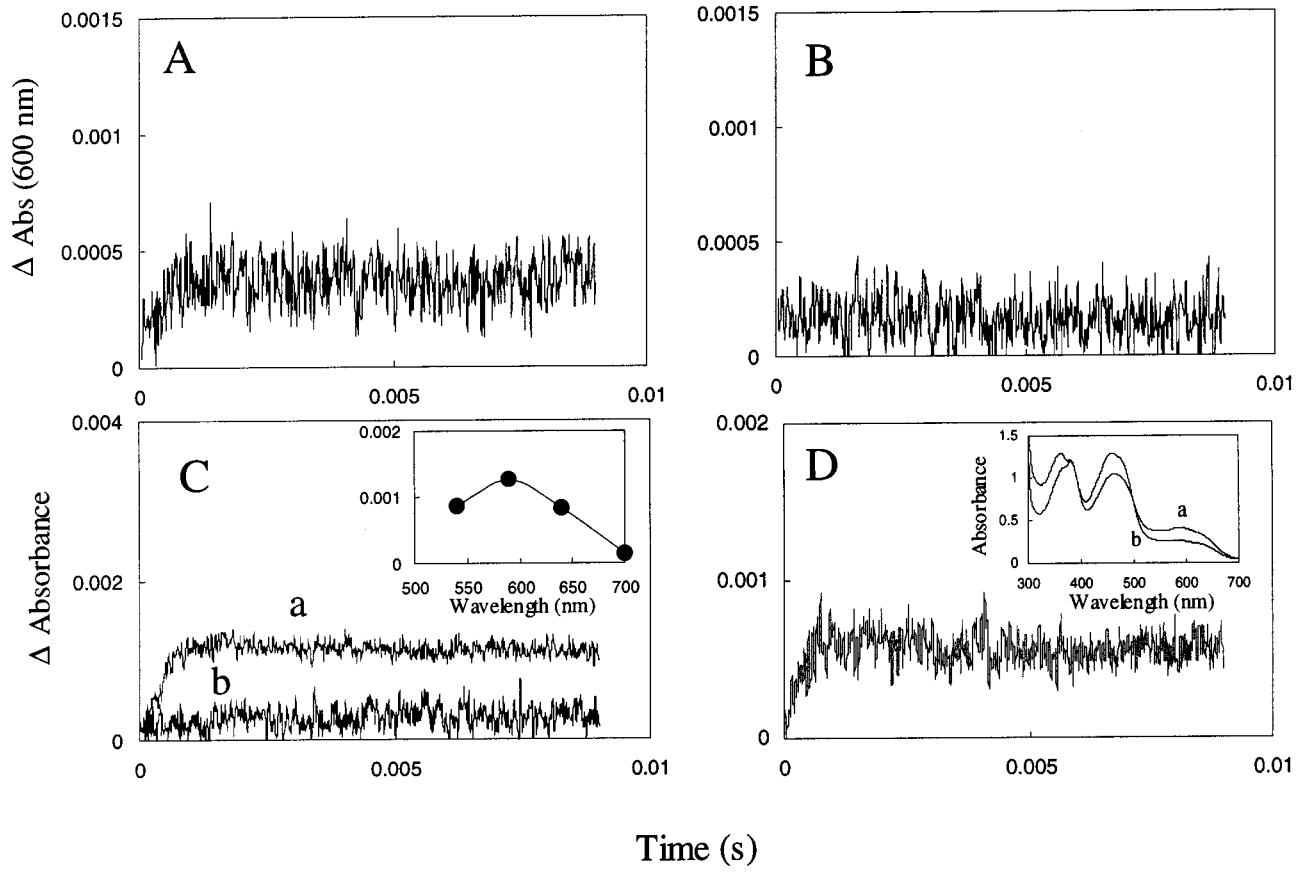

FIGURE 6: Absorption difference kinetic transients observed over short time base (10 ms). Conditions: 140 μM CPR, 100 mM potassium phosphate buffer, pH 7.0; temperature-jump as for Figure 4. Panel A: difference absorption transient at 600 nm for CPR reduced at the two-electron level with NADPH; $1/\tau = 1800 \pm 200$ s^{-1}. Panel B: as for panel A, but with CPR reduced at the two-electron level with sodium dithionite. Panel C: difference absorption transients observed for CPR reduced with excess nicotinamide cofactor [10-fold excess NADPH and NADP$^+$ (1.4 mM)]. Difference absorption transients 'a' and 'b' at 590 and 700 nm, respectively. Inset: kinetic difference spectrum generated by performing temperature-jump experiments at 540, 590, 640, and 700 nm. Panel D: difference absorption transient at 600 nm for CPR reduced with stoichiometric NADPH in the presence of 10-fold excess NADP$^+$. Inset: absorption spectrum of CPR in the presence of nicotinamide coenzymes. Spectrum 'a', in the presence of stoichiometric NADPH plus 10-fold molar excess NADP$^+$; spectrum 'b', in the presence of stoichiometric NADPH.

rium position of NADP$^+$ in the two-electron-reduced enzyme is that observed in the reported crystal structure—i.e., the nicotinamide ring is not tightly associated with the enzyme and is distant from the isoallozaxine ring of the FAD (*7*).

Forward and Reverse Interflavin Electron Transfer in CPR. The very low midpoint potential for the $FAD_{sq/hq}$ couple (−380 mV) precludes full reduction of CPR by NADPH even when the latter is present in large excess (Figure 7A). Under these conditions, the equilibrium favors electron transfer from FAD_{hq} to NADP$^+$, and the enzyme most probably exists in an equilibrium of states populated predominantly by the three-electron-reduced state (FAD_{sq}/FMN_{hq}) and to a lesser extent by the four-electron-reduced dihydroquinone state (FAD_{hq}/FMN_{hq}). Temperature-jump experiments with CPR samples equilibrated with a 10-fold molar excess of NADPH produced kinetic transients at 450 nm in which the absorption increased across the accessible time domain ($1/\tau = 20 \pm 0.2$ s^{-1}; Figure 7B); this contrasts with the 'up−down' transients observed for CPR reduced at the two-electron level (Figure 5A). Similar observations were made at 600 nm in the presence of excess NADPH (data not shown). The amplitude of the transient observed with excess NADPH decreases as the nicotinamide concentration is lowered, and eventually the trend reverses to yield the reduction in absorbance at stoichiometric NADPH (Figure 7C). We conclude that the kinetic phase observed with excess NADPH represents reverse electron transfer; the initial species is CPR containing FAD_{sq}/FMN_{hq}, and following the temperature-jump, the equilibrium is transiently shifted in favor of the FAD_{hq}/FMN_{sq} species. Our temperature-jump experiments have thus enabled us to measure the rate ($1/\tau = 20 \pm 0.2$ s^{-1}) of reverse electron transfer ($FAD_{sq}/FMN_{hq} \rightarrow FAD_{hq}/FMN_{sq}$) in three-electron-reduced enzyme and the observed rate ($1/\tau = 55 \pm 2$ s^{-1}) of forward electron transfer ($FAD_{sq}/FMN_{sq} \rightarrow FAD_{ox}/FMN_{hq}$) in two-electron-reduced enzyme. Supporting these assignments is the observed tradeoff between forward and reverse rates revealed in experiments with the W676H mutant CPR (see below).

The Potential Role of Gating in Interflavin Electron Transfer. The close proximity of the two flavin cofactors in the crystal structure of rat CPR suggests that interflavin electron transfer should be relatively fast (Figure 1). Using Dutton's electron-transfer rate ruler (*31*), we calculate an intrinsic electron-transfer rate of $\sim 3 \times 10^{10}$ s^{-1} for a separation distance of 4 Å, a driving force of −0.23 kcal·mol^{-1} (for a 10 mV separation in the respective flavin couples), and a typical reorganizational energy, λ, of 0.7 eV. The measured rates of internal electron transfer in human CPR are clearly much less than those calculated from electron-transfer theory, and similar to the rate measured in

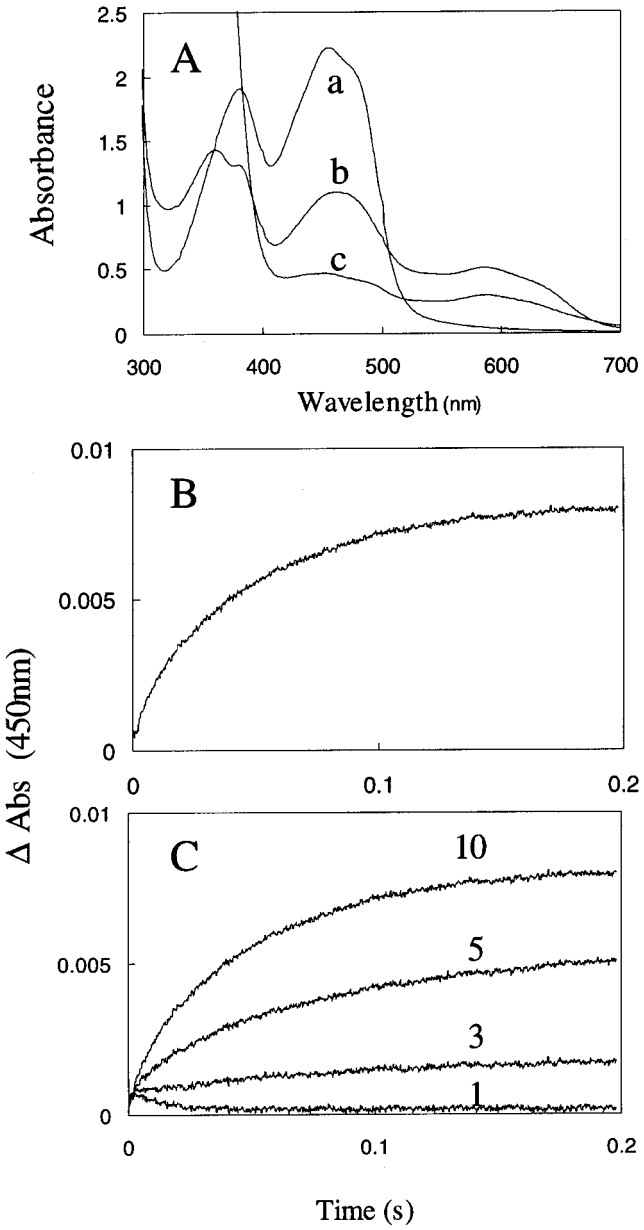

FIGURE 7: Relaxation transients observed with CPR reduced with a 10-fold molar excess of NADPH. Conditions: 140 μM CPR, 1.4 mM NADPH, 100 mM potassium phosphate buffer, pH 7.0; temperature-jump as for Figure 4. Panel A: spectrum 'a', absorption spectrum of oxidized CPR; spectrum 'b', absorption spectrum of CPR reduced at the two-electron level with NADPH; spectrum 'c', absorption spectrum of CPR reduced with a 10-fold molar excess NADPH—note incomplete reduction of the enzyme. Panel B: difference temperature-jump absorption transient for CPR reduced with a 10-fold molar excess of NADPH. The transient is best fitted to a single-exponential process ($1/\tau = 20 \pm 0.2$ s^{-1}). The amplitude change is 10-fold larger than those observed with two-electron reduced CPR. Panel C: progression from 'downward' to 'upward' transients on increasing the molar ratio of NADPH to CPR (numbers refer to the molar excess of NADPH).

one-electron-reduced rat CPR by using flavin photochemistry (*30*). Potential gating mechanisms need therefore to be explored.

In CPR, the neutral (blue) semiquinone is an observable catalytically competent intermediate. In temperature-jump experiments with two-electron-reduced CPR, one electron is transferred from FAD_{sq} to FMN_{sq} to form FAD_{ox} and FMN_{hq}. The blue semiquinone species is protonated at the

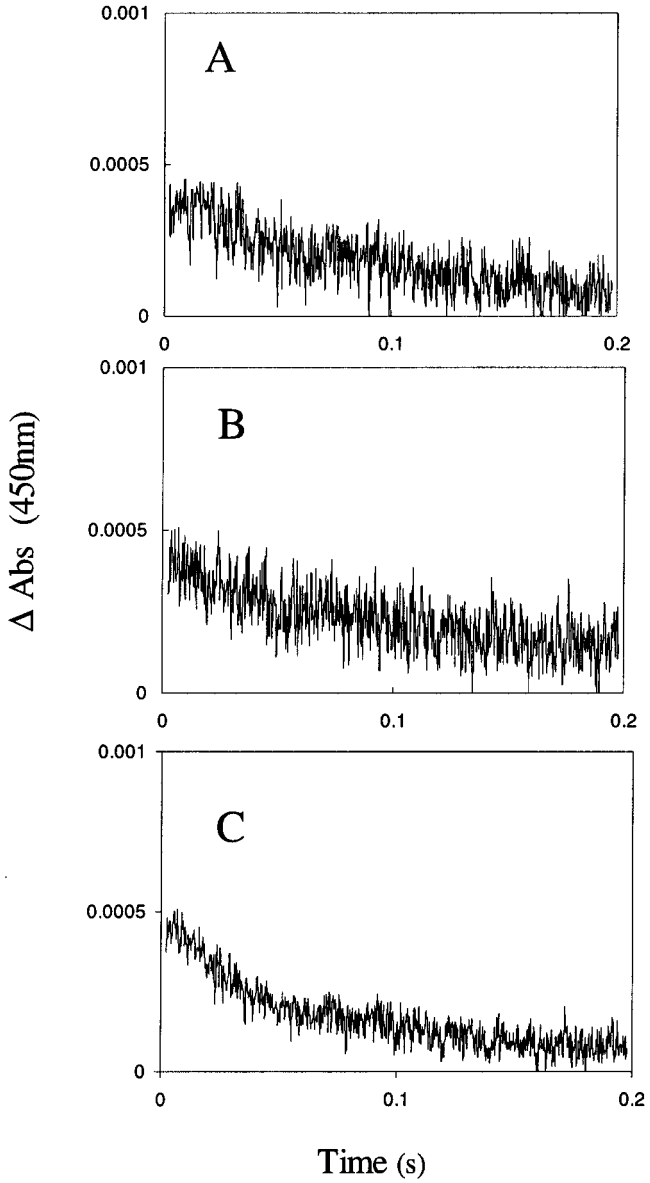

FIGURE 8: Difference absorption transients observed in deuterated solvent. Conditions: 140 μM CPR reduced to the two-electron level with sodium dithionite, 100 mM potassium phosphate buffer, pH 7.0; temperature-jump as for Figure 4. Panels A, B, and C are for experiments carried out at pD values 6.5, 7.0, and 7.5, respectively. Rates: panel A, $1/\tau = 11 \pm 2.8$ s^{-1}; panel B, $1/\tau = 10 \pm 4.3$ s^{-1}; panel C, $1/\tau = 19 \pm 1.6$ s^{-1}.

flavin N5 ($pK_a \sim 8$), necessitating deprotonation of the flavin prior to electron transfer. If the rate of this deprotonation were to be limiting for electron transfer, an isotope effect on the rate of electron transfer would be observed when carrying out the experiment in ^2H_2O. No such kinetic isotope effects were observed in temperature perturbation transients with CPR reduced at the two-electron level by sodium dithionite in 100% ^2H_2O at pD 6.5, 7.0, or 7.5 (Figure 8). These observations rule out any prototropic control of internal electron transfer in CPR.

The multidomain structure of CPR, with two catalytic domains, the FAD/NADPH-binding domain and the FMN-binding domain, linked by a 155 residue 'hinge domain', suggests the solution structure of the enzyme may be highly dynamic. The potential for domain rearrangements in CPR was noted very early (*7*), and subsequent structural and

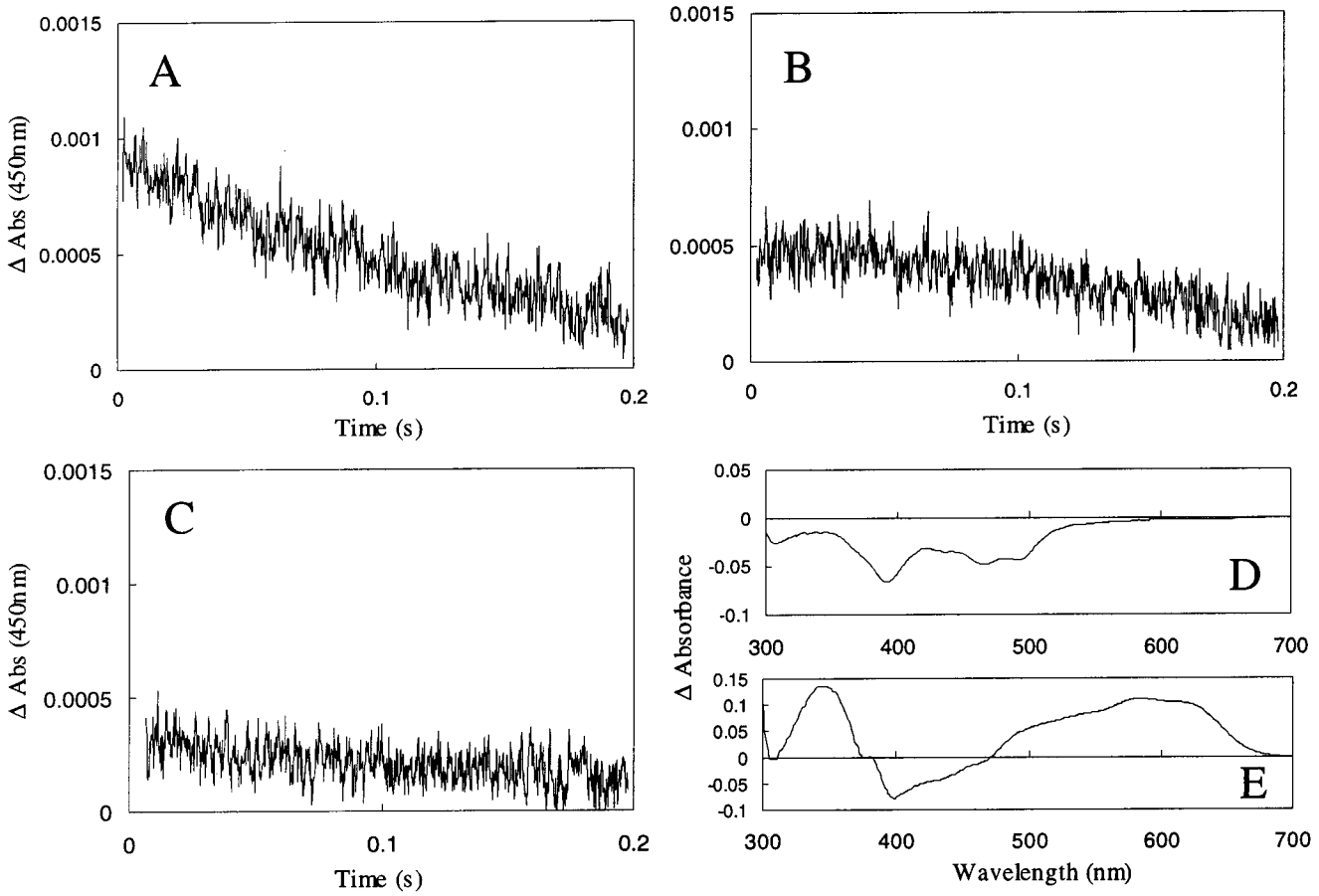

FIGURE 9: Effect of glycerol on the difference absorption transient for internal electron transfer in CPR reduced at the two-electron level with sodium dithionite. Panel A: difference absorption transients in the presence of glycerol (40% w/v). Panel B: difference absorption transients in the presence of glycerol (60% w/v). Panel C: difference absorption transients in the presence of glycerol (75% w/v). Panel D: Difference absorption spectrum [spectrum in the presence of glycerol (75% w/v) minus spectrum in the absence of glycerol] of oxidized CPR (50 μM). Panel E: Difference absorption spectrum [spectrum in the presence of glycerol (75% w/v) minus spectrum in the absence of glycerol] of CPR (100 μM) reduced at the two-electron level with dithionite.

mutagenesis studies have provided support for this idea (*32*−*34*). We have therefore examined the possibility that conformational events involving domain mobility might underlie the gating mechanism for internal electron transfer. Electrostatic interactions have been implicated in a 'domain swinging' model for electron transfer in CPR (*32*). We conjectured that increasing the ionic strength of CPR might interfere with these putative electrostatic interactions, but we found that addition of up to 300 mM KCl in the temperature-jump experiment did not affect the observed rate of interflavin electron transfer in CPR reduced to the two-electron level with dithionite ($1/\tau = 14 \pm 0.6$ and 11 ± 0.5 s^{-1} in the presence and absence of KCl, respectively; data not shown). This suggests that the properties of the hinge domain per se may be more important than any electrostatic interactions between the FAD/NADPH-binding domain and the FMN-binding domain in producing a productive mutual orientation of the two catalytic domains.

The motions of proteins and protein segments or domains can be hindered by hydrodynamic friction brought about by viscosogens (*35*−*37*). By contrast with the lack of ionic strength dependence, the observed relaxation rates are markedly sensitive to solvent viscosity (Figure 9). Increasing the glycerol concentration progressively diminishes the observed rate of electron transfer; at 75% (w/v) glycerol (an increase of ~50 in relative viscosity compared with solutions in the absence of glycerol), electron transfer is almost completely inhibited. This observation suggests that domain movements in CPR may play a major role in the mechanism of interflavin electron transfer. It is worth noting that high glycerol concentrations induce changes in the optical spectra of both oxidized and dithionite-reduced CPR samples (Figure 9B,C), indicative of changes in the average flavin environments. This further suggests that increasing glycerol concentrations may alter the equilibrium distribution of the different conformational states of CPR as well as the rate(s) of interconversion between them. These observations may also account for the smaller amplitudes in the absorption transients observed in t-jump experiments performed in the presence of glycerol.

The Role of Trp-676 in Interdomain Electron Transfer. A striking feature of the FNR family of flavoproteins is the existence of a highly conserved aromatic residue (W676 in human CPR) stacked against the *re*-face of the FAD isoalloxazine ring. This residue sterically interferes with the approach of the nicotinamide ring of NADPH to the isoalloxazine ring of FAD required for hydride transfer (Figure 1). We demonstrated previously that hydride transfer is accompanied by (and presumably requires) a series of conformational changes that affect the local environment of Trp-676. Removal of the indole ring in the W676H mutant significantly decreases the rate of nicotinamide coenzyme

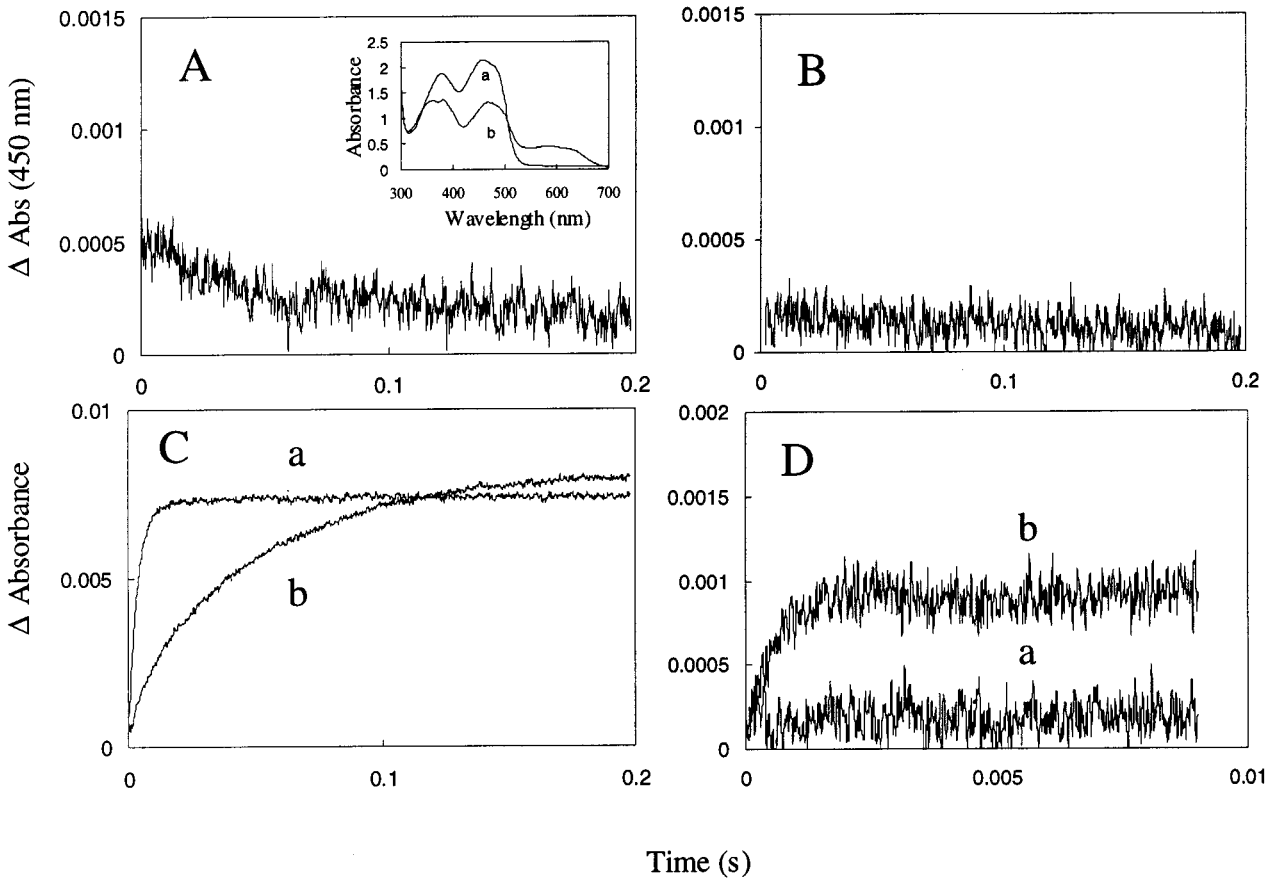

FIGURE 10: Temperature-jump studies with the W676H mutant of CPR. Conditions: 140 μM CPR W676H, 100 mM potassium phosphate buffer, pH 7.0; temperature-jump as for Figure 4. Panel A: difference absorption transient at 450 nm observed for CPR W676H reduced at the two-electron level with NADPH; $1/\tau = 27 \pm 1$ s^{-1}. Inset: spectrum of CPR W676H reduced at the two-electron level with NADPH. Panel B: as for panel A, but for CPR W676H reduced at the two-electron level with sodium dithionite. Panel C: as for panel A, but with enzyme reduced with a 10-fold molar excess of NADPH. Transient 'a' for CPR W676H ($1/\tau = 263 \pm 3$ s^{-1}); transient 'b' for wild-type CPR ($1/\tau = 20 \pm 0.2$ s^{-1}). Panel D: difference absorption transients at 600 nm over a short time base (10 ms) for wild-type and CPR W676H in the presence of excess nicotinamide cofactor (10-fold NADPH plus 10-fold NADP$^+$). Transient 'a', CPR W676H; transient 'b', wild-type CPR.

release following hydride transfer (*24*), giving rise to a new charge-transfer complex species (EH_2-NADP^+), not seen in wild-type CPR. This slow product release hinders the binding of a subsequent NADPH molecule and hence the turnover of the enzyme. Formation of this charge-transfer complex is reversible, and the mutant can thus be titrated with NADPH, albeit more slowly than the wild-type enzyme, prior to performing temperature-jump experiments. The absorption spectrum of the two-electron-reduced CPR W676H differs only slightly from that of the wild-type enzyme, displaying similar levels of flavin reduction and the blue semiquinone signature (Figure 10A, inset). In temperature-jump experiments with enzyme reduced to the two-electron level with NADPH, the observed rate for interflavin electron transfer ($FAD_{sq}/FMN_{sq} \rightarrow FAD_{ox}/FMN_{hq}$; $1/\tau = 27 \pm 1$ s^{-1}, Figure 10A) is a factor of 2 less than the corresponding rate ($1/\tau = 55 \pm 2$ s^{-1}) for wild-type CPR. This kinetic transient is completely lost in dithionite-reduced W676H CPR (Figure 10B).[3] However, contrasting with this decrease in the forward observed rate of electron transfer, we observed a ~13-fold *increase* in the rate of electron transfer in the reverse direction ($FAD_{sq}/FMN_{hq} \rightarrow FAD_{hq}/FMN_{sq}$; $1/\tau = 263 \pm 3$ s^{-1}, Figure 10C) for enzyme reduced with a 10-fold excess of NADPH. The effect of the mutation is thus to shift the balance between the forward and reverse electron-transfer rates to favor the latter process. The mechanism by which the interaction of Trp-676 with FAD favors the physiological direction for interflavin electron transfer will need to be addressed in future work.

Interestingly, the relaxation transients for NADPH-reduced W676H (obtained by incubating with a 10-fold molar excess of NADPH and NADP$^+$) do not show the initial 'up' phase observed for the wild-type enzyme (Figure 10D). This observation clearly confirms that this initial phase does not represent interflavin electron transfer and strengthens our conclusion that it is associated with local conformational changes around the FAD. It further suggests that these changes involve movement of the C-terminal tryptophan residue.

DISCUSSION

The measurement of the rates of internal electron movements in proteins with multiple redox centers is technically challenging and, owing to rate limitation by preceding kinetic steps (e.g., a chemical conversion), is often not possible using conventional stopped-flow kinetic methods. Alternative kinetic methods [flash photolysis (*38*) and equilibrium

[3] Owing to the time course of cooling after the temperature jump, it was not possible to extend the time base beyond 200 ms to obtain evidence for slower kinetic phases.

perturbation methods (*39*)] remove the constraints imposed by the stopped-flow method, and allow direct access to internal electron-transfer reactions. Our previous stopped-flow studies with human CPR indicated that flavin reduction ($k \sim 20$ s^{-1} under pseudo-first-order conditions) limits the rate of internal electron transfer from FAD to FMN (*21*). We have now demonstrated in stopped-flow studies with stoichiometric NADPH that the rate of flavin reduction and formation of the blue semiquinone form of CPR occurs at a rate of ~70 s^{-1} (see Figure 2 for the blue semiquinone signal; similar transients were observed in the fluorescence mode for NADPH oxidation). Under these conditions, the rate of flavin reduction is not suppressed by the binding of a second molecule of NADPH to the noncatalytic coenzyme-binding site that we identified in our previous work (*21*). To investigate the rate of interflavin electron transfer in CPR, and to establish whether this is gated by flavin reduction or by other processes, a new method for measuring the rates of internal electron transfer is required. We have developed such a method using a temperature-jump approach, which frees us from the limitations of the stopped-flow method; this has allowed us to measure directly the rates of internal electron transfer in two-electron- and three-electron-reduced CPR.

Our temperature-jump measurements indicate that the observed rate ($1/\tau = 55 \pm 2$ s^{-1}) of internal electron transfer ($FAD_{sq}FMN_{sq} \rightarrow FAD_{ox}FMN_{hq}$) in two-electron-reduced CPR is comparable to that of flavin reduction (~70 s^{-1} for CPR reduced with stoichiometric NADPH). Data collected at 450 and 600 nm are consistent with the electron movement shown in Scheme 1; as discussed above, a range of evidence rules out the possibility that the fast phase ($1/\tau = 2200 \pm 300$ s^{-1}) of absorbance change in experiments with NADPH-reduced CPR is a redox process. The observed rate ($1/\tau = 55 \pm 2$ s^{-1}) of electron transfer in human CPR is similar to that reported (70 s^{-1}) for internal electron transfer in rabbit CPR, measured by flash photolysis methods (*30*). However, the flash photolysis approach rapidly reduces CPR to the one-electron level; the value of 70 s^{-1} therefore represents electron transfer in one-electron-reduced enzyme rather than the two-electron-reduced CPR studied in our temperature-jump experiments. In the flash photolysis experiment, the driving force for transfer of an electron from FAD_{sq} to FMN_{ox} will be large [180 mV (*23*)], whereas in the temperature-jump experiments the initial equilibrium is poised at ~50:50 [consistent with potentiometry studies of human CPR (*22*); Scheme 1], and the driving force following a temperature-jump will be relatively small. Reduction of rabbit CPR to the one-electron level prior to performing flash photolysis yields a rate for internal electron transfer of 15 s^{-1} (*30*). In this experiment, the electron-transfer reaction ($FAD_{sq}FMN_{sq} \rightarrow FAD_{ox}FMN_{hq}$) is the same as that in our temperature-jump analyses; the modest difference in the measured rates no doubt reflects species differences between the two CPR enzymes.

The finding that the observed rates of internal electron transfer in one-electron-reduced and two-electron-reduced CPR are similar, and substantially less than that predicted by electron-transfer theory, suggests the reaction is kinetically restricted by additional adiabatic processes (i.e., the reaction is gated). The findings that the rate is decreased by inclusion of glycerol, but not in deuterated solvent, suggest that this reaction is limited by conformational change and not by deprotonation of groups in the enzyme. This conformational gating of electron transfer in CPR is likely to result from the kind of domain movements which have been inferred from recent crystallographic studies of mutants of rat CPR with substitutions in the region of the nicotinamide cofactor binding site, where differences were observed in the spatial juxtaposition of the FAD- and FMN-binding domains (*33*). Similar 'disorder' in the position of the FMN-binding domain has been observed in other members of the family of diflavin reductases (*40*).

Our temperature-jump experiments performed with enzyme reduced to the two-electron level either by NADPH or by dithionite indicate that the presence of nicotinamide coenzyme in the active site of CPR enhances the rate of electron transfer from FAD_{sq} to FMN_{sq}. Two possible mechanisms could account for this observation: (i) nicotinamide coenzyme-induced perturbation of the flavin (FAD) potential and/or (ii) a conformational change on coenzyme binding that enhances electronic coupling between the flavin cofactors. In this paper, we did not observe a change in tryptophan fluorescence on performing the temperature-jump experiment, or obtain evidence for a reduced enzyme−$NADP^+$ charge-transfer complex. However, in our stopped-flow studies of human CPR, rapid mixing of enzyme with NADPH gave rise to substantial changes in tryptophan fluorescence (*21*). Subsequent analysis using the W676H mutant of CPR demonstrated that these changes are attributed to a movement of Trp-676 (*24*). This leads us to conclude that under the conditions of the temperature-jump experiment there is no movement of Trp-676 of the kind induced by the binding of the nicotinamide ring of the coenzyme. It follows that in two-electron-reduced CPR, the NMN portion of $NADP^+$ is likely to be in the position, somewhat distant from the FAD isoalloxazine ring, observed in the crystal structure of oxidized rat CPR (*7*), making it improbable that the presence of $NADP^+$ has any substantial effect on the redox potential of FAD. We propose, therefore, that the enhancement of the rate of internal electron transfer observed in temperature-jump experiments with coenzyme-reduced CPR can be attributed to a conformational change on coenzyme binding. This conformational change may be restricted to the FAD domain, or indeed may influence the relative positioning of the FAD- and FMN-binding domains.

Our temperature-jump experiments have also enabled us, for the first time, to measure the rate of electron transfer in the reverse direction ($FAD_{sq}FMN_{hq} \rightarrow FAD_{hq}FMN_{sq}$; $1/\tau = 20 \pm 0.2$ s^{-1}) in three-electron-reduced CPR. In the W676H mutant of CPR, this rate of reverse electron transfer is substantially increased ($1/\tau = 263 \pm 3$ s^{-1}), whereas the 'forward' rate ($FAD_{sq}FMN_{sq} \rightarrow FAD_{ox}FMN_{hq}$) for CPR W676H is decreased by only a factor of ~2 ($1/\tau = 27 \pm 1$ s^{-1}). This implies that the presence of the W676 residue in wild-type CPR favors electron transfer in the physiological direction. The mechanistic basis for this directional control on the internal electron-transfer reactions in CPR is unknown. However, it is worth noting that in *Anabaena* flavodoxin the replacement of Trp-57, which stacks over the FMN, with a nonaromatic residues (Ala or Leu) increases the reduction potential of the $FMN_{sq/hq}$ couple, by around 30 mV (*41*). Our reductive titrations of W676H CPR also indicate that in the equilibrium mixture containing two-electron-reduced enzyme

the absorption at 600 nm corresponding to the blue semiquinone form is slightly reduced compared with wild-type CPR. Combined, these observations suggest that the potential of the $FAD_{sq/hq}$ couple in W676H CPR may be somewhat elevated compared with the same couple in wild-type CPR.

In summary, the temperature-jump method has opened up studies of internal electron transfer in CPR in a way previously not possible using conventional stopped-flow approaches. Our approach could, in principle, be extended to other members of the diflavin reductase family of enzymes in which potentiometric measurements indicate that an equilibrium distribution of enzyme forms exists in two- or three-electron-reduced states. Our attention is now focused on using the temperature-jump method to elucidate the mechanism(s) of enhancement of the rate of electron transfer by coenzyme binding in CPR and in mutants of CPR with substitutions in the nicotinamide coenzyme binding site, with the aim of understanding at the atomic level the link between protein conformational change and the mechanism of internal electron transfer.

ACKNOWLEDGMENT

We thank Alex Grunau for skilled technical assistance, Dr. Carol Baxter for assistance in preparing Figure 1, and Dr. Clive Bagshaw for advice on experimental methods.

REFERENCES

1. Strobel, H., Hodgson, A., and Shen, S. (1995) in *Cytochrome P450: Structure, Mechanism and Biochemistry* (Ortiz de Montellano, P., Ed.) pp 225−244, Plenum Press, New York.
2. Philips, A., and Langdon, R. (1962) *J. Biol. Chem. 237*, 2652−2660.
3. Lu, A., Junk, K., and Coon, M. (1969) *J. Biol. Chem. 244*, 3714−3721.
4. Porter, T. D. (1991) *Trends Biochem. Sci. 16*, 154−158.
5. Shen, A., and Kasper, C. B. (1993) in *Handbook of Experimental Pharmacology* (Schenkman, J. B., and Grein, H., Eds.) pp 35−59, Springer-Verlag, New York.
6. Iyanagi, T., and Mason, H. S. (1973) *Biochemistry 12*, 2297−2307.
7. Wang, M., Roberts, D. L., Paschke, R., Shea, T. M., Masters, B. S., and Kim, J. J. (1997) *Proc. Natl. Acad. Sci. U.S.A. 94*, 8411−8416.
8. Enoch, H. G., and Strittmatter, P. (1979) *J. Biol. Chem. 254*, 8976−8981.
9. Schacter, B. A., Nelson, E. B., Marver, H. S., and Masters, B. S. (1972) *J. Biol. Chem. 247*, 3601−3607.
10. Ilan, Z., Ilan, R., and Cinti, D. L. (1981) *J. Biol. Chem. 256*, 10066−10072.
11. Masters, B. S. S. (1980) in *Enzymatic basis of detoxification* (Jakoby, W., Ed.) pp 183−200, Academic Press, Inc., Orlando, FL.
12. Kurzban, G. P., and Strobel, H. W. (1986) *J. Biol. Chem. 261*, 7824−7830.
13. Keyes, S. R., Fracasso, P. M., Heimbrook, D. C., Rockwell, S., Sligar, S. G., and Sartorelli, A. C. (1984) *Cancer Res. 44*, 5638−5643.
14. Bligh, H. F., Bartoszek, A., Robson, C. N., Hickson, I. D., Kasper, C. B., Beggs, J. D., and Wolf, C. R. (1990) *Cancer Res. 50*, 7789−7792.
15. Bartoszek, A., and Wolf, C. R. (1992) *Biochem. Pharmacol. 43*, 1449−1457.
16. Walton, M. I., Wolf, C. R., and Workman, P. (1992) *Biochem. Pharmacol. 44*, 251−259.
17. Patterson, A. V., Barham, H. M., Chinje, E. C., Adams, G. E., Harris, A. L., and Stratford, I. J. (1995) *Br. J. Cancer 72*, 1144−1150.
18. Griffith, O. W., and Stuehr, D. J. (1995) *Annu. Rev. Physiol. 57*, 707−736.
19. Leclerc, D., Wilson, A., Dumas, R., Gafuik, C., Song, D., Watkins, D., Heng, H. H., Rommens, J. M., Scherer, S. W., Rosenblatt, D. S., and Gravel, R. A. (1998) *Proc. Natl. Acad. Sci. U.S.A. 95*, 3059−3064.
20. Paine, M. J., Garner, A. P., Powell, D., Sibbald, J., Sales, M., Pratt, N., Smith, T., Tew, D. G., and Wolf, C. R. (2000) *J. Biol. Chem. 275*, 1471−1478.
21. Gutierrez, A., Lian, L. Y., Wolf, C. R., Scrutton, N. S., and Roberts, G. C. (2001) *Biochemistry 40*, 1964−1975.
22. Munro, A. W., Noble, M. A., Robledo, L., Daff, S. N., and Chapman, S. K. (2001) *Biochemistry 40*, 1956−1963.
23. Oprian, D. D., and Coon, M. J. (1982) *J. Biol. Chem. 257*, 8935−8944.
24. Gutierrez, A., Doehr, O., Paine, M., Wolf, C. R., Scrutton, N. S., and Roberts, G. C. (2000) *Biochemistry 39*, 15990−15999.
25. *T-jump users guide*, p 4, Hi-Tech Scientific, Salisbury, U.K.
26. Deng, H., Zhadin, N., and Callender, R. (2001) *Biochemistry 40*, 3767−3773.
27. Urbanke, C., and Wray, J. (2001) *Biochem. J. 358*, 165−173.
28. Hiromi, K. (1979) in *Kinetics of fast enzyme reactions*, pp 147−148, Kodansha/Wiley & Sons, Tokyo/New York.
29. Turner, D. (1986) in *Investigations of rates and mechanisms of reactions. Part II* (Bernasconi, C., Ed.) 4th ed., p 147, John Wiley & Sons, New York.
30. Bhattacharyya, A. K., Lipka, J. J., Waskell, L., and Tollin, G. (1991) *Biochemistry 30*, 759−765.
31. Page, C. C., Moser, C. C., Chen, X., and Dutton, P. L. (1999) *Nature 402*, 47−52.
32. Zhao, Q., Modi, S., Smith, G., Paine, M., McDonagh, P. D., Wolf, C. R., Tew, D., Lian, L. Y., Roberts, G. C. K., and Driessen, H. P. (1999) *Protein Sci. 8*, 298−306.
33. Hubbard, P. A., Shen, A. L., Paschke, R., Kasper, C. B., and Kim, J. J. (2001) *J. Biol. Chem. 276*, 29163−29170.
34. Hall, D. A., Vander Kooi, C. W., Stasik, C. N., Stevens, S. Y., Zuiderweg, E. R., and Matthews, R. G. (2001) *Proc. Natl. Acad. Sci. U.S.A. 98*, 9521−9526.
35. Qin, L., and Kostic, N. M. (1994) *Biochemistry 33*, 12592−12599.
36. Clarke, A. R., Waldman, A. D., Hart, K. W., and Holbrook, J. J. (1985) *Biochim. Biophys. Acta 829*, 397−407.
37. Gurfreund, H. (1995) *Kinetics in the Life Sciences*, pp 248−261, Cambridge University Press, Cambridge, U.K.
38. Tollin, G. (1995) *J. Bioenerg. Biomembr. 27*, 303−309.
39. Tegoni, M., Silvestrini, M. C., Guigliarelli, B., Asso, M., Brunori, M., and Bertrand, P. (1998) *Biochemistry 37*, 12761−12771.
40. Gruez, A., Pignol, D., Zeghouf, M., Coves, J., Fontecave, M., Ferrer, J. L., and Fontecilla-Camps, J. C. (2000) *J. Mol. Biol. 299*, 199−212.
41. Lostao, A., Gomez-Moreno, C., Mayhew, S. G., and Sancho, J. (1997) *Biochemistry 36*, 14334−14344.

BI0159433